ON THE FRACTALITY OF BASIN BOUNDARIES*

J. PEINKE[1], M. KLEIN[2], J. PARISI[3], A. KITTEL[4]

AND

O.E. ROESSLER[2]

[1] C.N.R.S. - C.R.T.B.T., B.P. 166
F-38042 Grenoble Cedex 9, France

[2] Institute for Physical and Theoretical Chemistry
University of Tübingen
D-W-7400 Tübingen, FRG

[3] Physics Institute, University of Zurich
Schönberggasse 9, CH - 8001 Zurich, Switzerland

[4] Physical Institute, University of Tübingen
D-W-7400 Tübingen, FRG

(Received March 3, 1992)

Fractal structures arising in basin boundaries are discussed. A brief survey on properties of Julia, Fatou, and Mandelbrot sets is given. The meaning of analyticity is investigated by means of perturbations which destroy analyticity. A nonanalytic map is quoted which generates the same fractal structures like the complex logistic map. It is shown that the fractality of basin boundaries is generated by chaotic forcing of a bistability. A generic model is given for this simple mechanism. An explicit expression for the fractal boundary is deduced for this approach and it is interpreted as a new model system generating structures with similar properties as known from turbulence.

PACS numbers: 05.45. +b, 03.40. Gc

---

* Presented at the IV Symposium on Statistical Physics, Zakopane, Poland, September 19–29,1991.

1. Introduction

If one wants to write something about fractals, first of all one has to quote the work of Mandelbrot [1], who actualized the work of Julia [2] and Fatou [3], introduced the name "fractal", and showed the general meaning of fractals for nature. Another aspect of fascination has been irradiated by the work of Peitgen and Richter [4], exhibiting the beauty of fractals. Well, we want to start our paper with some comments on the beauty. We believe that a good part of the actual motivation to investigate fractals is coming from their beauty. Fractals are characterized by special, perfect interplay between the whole structure and details of the structure. The interplay seems to be also present in nature. Looking closer and closer at many natural structures, we find a harmonic interplay between details and the whole. The very subjective impression of beauty of fractals may be based on the fact that they unveil this natural harmony in a pure and abstract way. We, as human beings and thus as a part of nature, do not need to know a mathematical quantification of this natural harmony, but can feel it directly by looking at a structure. This is the point of fascination and beauty.

In this paper, we focus on fractals generated by discrete maps. We start out with complex analytic maps and their basin boundaries, well known as Julia sets. One essential aim of our work was to explain these structures of Julia sets by a simple model which can be set in connection with the way in which Newton described nature.

2. Complex analytic fractals

This part is devoted to fractals which are generated by complex analytic functions. For simplicity, only the complex logistic map

$$f_c(z) = z^2 + c \tag{1}$$

with $z, c \in \mathbb{C}$, is considered. The analyticity of this map is characterized by the fulfillment of the Chauchy–Riemann condition; taking $f_c = u + iv$ this condition is written like

$$\begin{aligned} \frac{du}{dx} &= \frac{dv}{dy}, \\ \frac{du}{dy} &= -\frac{dv}{dx}. \end{aligned} \tag{2}$$

In the following, some basic results on this function (1) will be reported. For an extended discussion, we refer to literature like [5,6]. It is amazing to

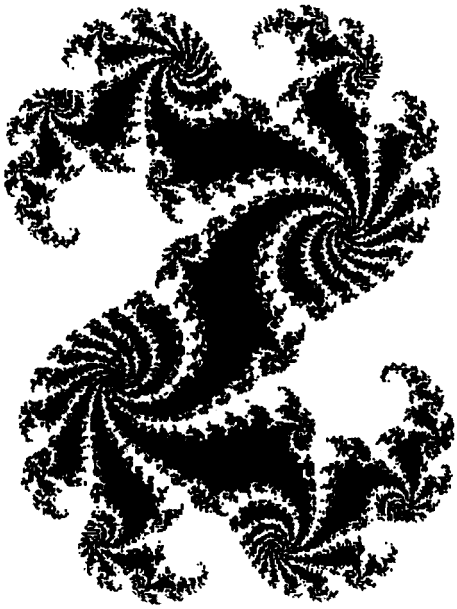

Fig. 1. Basin of attraction or filled-in Julia set for function (1) with $c = 0.32 + i\,0.043$. The x-axis was chosen to be $\mathrm{Re}\, z_0$ and the y-axis to be $\mathrm{Im}\, z_0$. Both times the corresponding component of z_0 was changed from -1.2 to 1.2; after [10].

see that such a simple equation may lead to very complex structures, like this one shown in Fig. 1.

The work on fractals of complex analytic functions is based on the works of Julia [2] and Fatou [3]. They investigated convergence properties of the families of functions $\{f^n\}$ generated by rational complex functions f. Here f^n denotes $f^n = f \cdot f^{(n-1)}$. The convergence of $\{f^n\}$ was investigated with respect to the chosen argument z of the complex plane. They found that the complex plane of z is divided up in subsets where either no convergence or some convergence exists. For the case of convergence (including convergence to infinity), the family was called to be normal on this subset. The set of convergent points z for a function f is called Fatou set. Thus, the following definition can be used: $z \in \mathbb{C} = \mathbb{C} \cup \{\infty\}$ is an element of the Fatou set $F(f)$ if there exists a neighborhood U of z in $\mathbb{C}$ such that the family $\{f^n|U\}$ is a normal family. The Julia set $J(f)$ is the complement of the Fatou set [6].

Nowadays, the families $\{f^n\}$ are interpreted in a more dynamical way. One takes the function $f^n(z)$ as the iteration of $f^{n-1}(z)$. This iteration is regarded as a process in time. Thus, the points $f^n(z)$ for $n > 0$ correspond to values of a variable $z(t)$ evolving in time but taken at some discrete time steps $t = n\tau$. This leads to the following notation: z_0 is the initial point

and may be written as

$$z_0 = f^0(z_0)$$

and

$$z_n = f^n(z_0).$$

The iteration is now

$$z_{n+1} = f(z_n). \tag{3}$$

In this context, the convergence of the family $\{f^n\}$ corresponds to the temporal evolution of an initial point z_0 under the iteration with f to a fixed point or to a periodic point. Thus, the Fatou set is the unification of all basins of attraction. Note, the basin of attraction of infinity is included. The complement of the Fatou set is, as already mentioned, the Julia set. Consequently, the Julia set J can be taken as the boundary of the basins of attraction. J is a repellor. Under iteration, points very close to J run away from J. It can be shown that the boundary of any single basin boundary is already the whole Julia set. This leads to very strange properties, if, for example, three different attractors exist. Here, J is always the boundary of all three basins of attraction. There is no boundary point where only two basins of attraction meet each other.

The numerical evaluation of the Julia and the Fatou set is easily achieved by using the properties just mentioned. The initial conditions of the complex plane are scanned over a region of $\mathbb{C}$. Each initial condition z_0 is iterated several times. (Usually 50 to 100 iterations are already sufficient to obtain very precise results.) The best way to evaluate these sets is to look for all initial points which converge to infinity. If for a value n the absolute value of z_n is larger than 3, z_n will go to infinity under further iteration, see Devany in [7]. In this way, we obtained Fig. 1 using function (1). The white points correspond to z_0 values which are attracted by infinity, and thus belong to the basin of attraction of infinity. Using the fact that the boundary of this basin is the Julia set, we say that the black points represent the filled-in Julia set. Actually, the Julia set corresponds to the boundary between the white and the black region.

To explain the Mandelbrot set, one special property of the iteration of $z_0 = 0$ (the critical point of the map) has to be regarded. For a chosen parameter value $c \in \mathbb{C}$ of the complex map $f_c(z) = z^2 + c$, the corresponding Julia set $J(f_c)$ may be connected or not. $J(f_c)$ is connected, if $z_0 = 0$ does not go to infinity under iteration, otherwise $J(f_c)$ is not connected. In the unconnected case, $J(f_c)$ corresponds to a Cantor dust. To obtain the Mandelbrot set, the parameter $c \in \mathbb{C}$ is scanned over a region in $\mathbb{C}$. For each chosen c value $z_0 = 0$ is iterated, and it is asked whether this initial value goes to infinity or not. In Fig. 2, the resulting Mandelbrot set is shown. The white points correspond to parameter values c for which $z_0 = 0$ goes

to infinity under iteration. The numerical evaluation of these structures is not at all difficult. Algorithms to generate these structures can be found in Refs. [4,8].

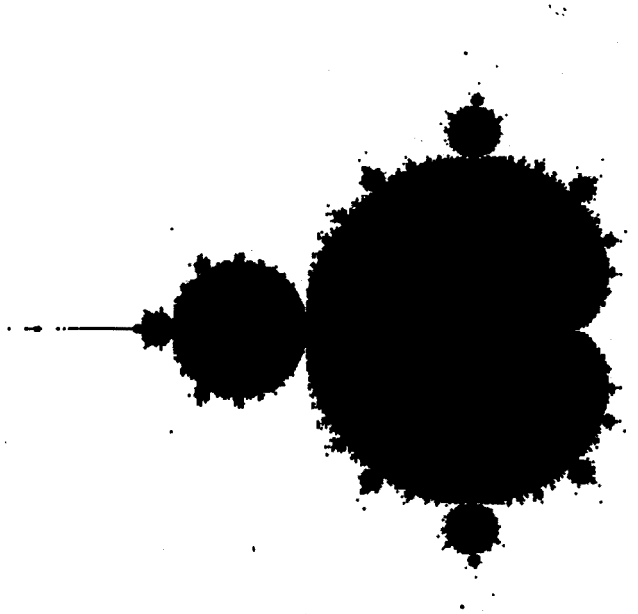

Fig. 2. Mandelbrot set. Shown is the complex plane of parameter values c of function (1). Along the x-axis the real part of c has been changed from -2.0 to 0.5; along the y-axis the imaginary part of c has been changed from -1.25 to 1.25; after [10].

Up to now, we have discussed some properties of complex analytic maps together with some nice illustrations. We have used the word fractals quite often without defining this word. Well, what is a fractal? Definitely, every reader has an idea of what a fractal is, and it is much easier and more pleasant to give some feeling of what a fractal is than to define it. Nevertheless, we want to precise in the following what fractal means. The images shown in Figs. 1 and 2 have the characteristic property that the magnification of small details reveals always new images with the same beauty. In the Julia sets, always similar structures are found under magnification. That is why they are called to be self-similar. On the other hand, always new structures are found in the Mandelbrot set under magnification, if the location is changed along the borderline. An interesting feature of these different local structures of the Mandelbrot set is that they correspond to the form of the corresponding Julia set. Keep in mind that each point of the Mandelbrot set corresponds to one value $c \in \mathbb{C}$ from which a Julia set can be constructed. Along the boundary of the Mandelbrot set, the Julia set encloses a very

small basin of attraction containing the point $z_0 = 0$. In the ideal case, the Julia sets must be a line, because within any ε neighborhood there are c values for which the Julia sets are only Cantor dusts. There does not any more exist a finite region of a basin of attraction for initial conditions which do not converge against infinity. This can be also expressed by saying that the basin of attraction for initial points not going to infinity has the measure zero.

The magnification property of fractals can be expressed by a scaling law. For a property **A** of this structure (well chosen) it holds that $A(\lambda x) = \lambda^{\alpha} A(x)$. If, for example, x is a typical length scale like the diameter of a disc, and A is the number of discs with this diameter necessary to cover this structure, the scaling exponent a corresponds to the Hausdorff dimension. If for a structure a is no integer, one says that this structure is a fractal. Structures with a simple geometry, like a line or a plane, have integer valued Hausdorff dimension. For a detailed discussion of fractals see also Ref. [9].

3. Nonanalytic fractals

Up to now, we have discussed only the mathematical background of the Julia, Fatou, and Mandelbrot set. For the definition of these sets of the complex plane the analyticity of the generating function was essential. Next, we want to turn our attention to the meaning of these mathematical features for the geometry of fractals.

Mandelbrot's idea is that fractals can be taken as an approximation to describe structures in nature. Here, the question arises whether complex analytic functions are necessary. If so, they would play a special role in nature. Or, is the mathematical property of complex analyticity only sufficient to generate fractals? From a classical point of view, *i.e.* based on Newton's philosophy to describe nature by unique, time invertible processes, we expect that the rational complex analytic functions are not appropriate. The existence of a critical point in these functions destroys the time reversibility in the mentioned dynamical interpretation. For a more extended discussion of this point see Ref. [10].

To get a first understanding of the meaning of analyticity, one may perturb equation (1) by a small nonanalytic term

$$f_c(z) = z^2 + c + \varepsilon \operatorname{Re}(z). \tag{4}$$

Here, ε is a small real number multiplied by the real part of z. Using the notations $z = x + iy$, $c = c_{\mathrm{re}} + ic_{\mathrm{im}}$, and $f = u + iv$, this equation has the following form

$$\begin{aligned} u_c(x, y) &= x^2 - y^2 + c_{\mathrm{re}} + \varepsilon x, \\ v_c(x, y) &= 2xy + c_{\mathrm{im}}. \end{aligned} \tag{5}$$

For equation (5), corresponding Julia sets can be evaluated in $\mathbb{C}$ or in $\mathbb{R}^2$, respectively [11-14]. In Fig. 3, an example of such a Julia set is shown. The basin of attraction of infinity is colored white. Investigating the structures of this corresponding Julia sets for the equation (5) by changing the value of the parameters c_{re} and c_{im}, similar structures of the original Julia sets of the complex logistic map (equation (1)) are found. The structure of Fig. 3 seems to be fractal, nowhere differentiable and self-similar. In contrast to these "wild" fractal structures, which can also be characterized as bifractals [15], sometimes the basin boundaries become locally smooth, see Fig. 4. Here, fractality is still present in the support of the bays.

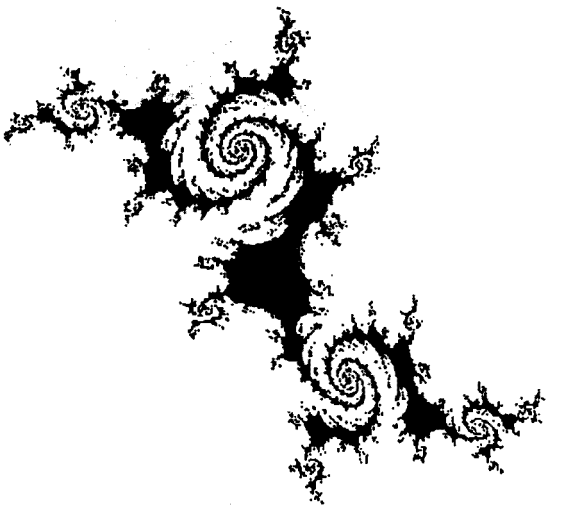

Fig. 3. Basin of attraction for equation (5) with $c_{re} = -0.03$, $c_{im} = 0.75$, and $\varepsilon = 0.3$; after [13].

Besides the structures in the plane of initial conditions (basin of attractions) one may also evaluate some structures in the plane of the control parameters c_{re} and c_{im}. Without taking care of the changed mathematics (for equation (4) there is now a whole set of critical points on a circle and nothing is known about the relation between the dynamics of the critical points and the form of the basin of attractions), one may construct a generalized Mandelbrot set just by applying the same method of the original Mandelbrot set. Fig. 5 clearly presents a distortion of the original Mandelbrot set. An interesting point is that the local structure of this generalized Mandelbrot set has again a similar geometry like the corresponding "generalized Julia set" of the corresponding parameter values. Here, compare the inset of Fig. 5 with Fig. 3. This similarity can be attributed to the following simple argument. In the Mandelbrot set a point is colored white if

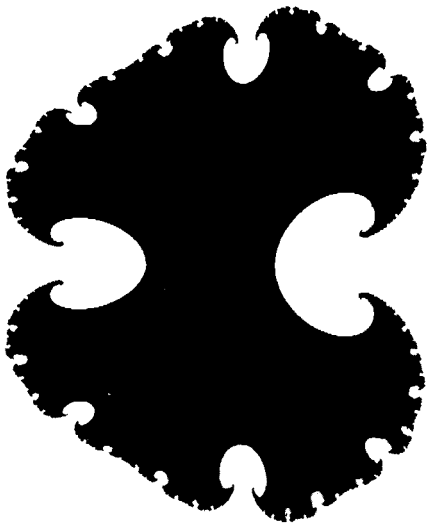

Fig. 4. Basin of attraction for equation (5) with $c_{re} = 0.12253920, c_{im} = 0.0$, and $\epsilon = 0.3$; after [14].

the iteration of one special initial point diverges to infinity, *i.e.*, this initial point lies in the white region of the corresponding (generalized) Julia set. Let us regard in the following the case of a point close to the boundary of the (generalized) Mandelbrot set. Here, the iterated initial point is also very close to the (generalized) Julia set, *i.e.*, it is close to the boundary of the basins of attraction. Changing the control parameters slightly, the form of (generalized) Julia sets is also changed slightly. Thus, the initial point may change its position from one basin of attraction to the other in the plane of initial conditions, this means that the initial point is one time inside and the next time outside of the (generalized) Julia set. As a result, the color in the (generalized) Mandelbrot set changes in a corresponding way. Thus, it seems to be natural that the fractal structure of a (generalized) Julia set is mapped onto the Mandelbrot set in the way like a scanning microscope works. To give a vivid description, the principle of this "scanning microscope" is the following: the beam point is kept fixed and the sample (the (generalized) Julia set) is "moved" (deformed) due to changes of the parameters c_{re} and c_{im}. The detected structure (the (generalized) Mandelbrot set) is obtained by the feature whether the beam point is inside or outside the (generalized) Julia set. The same arguments can be thought over for the "less fractal" structure of Fig. 4. The corresponding local structure of the generalized Mandelbrot set is at the right notch and it is smooth.

As a last point we want to mention that the Mandelbrot set and all Julia sets of the complex analytic equation (1) can also be generated by the

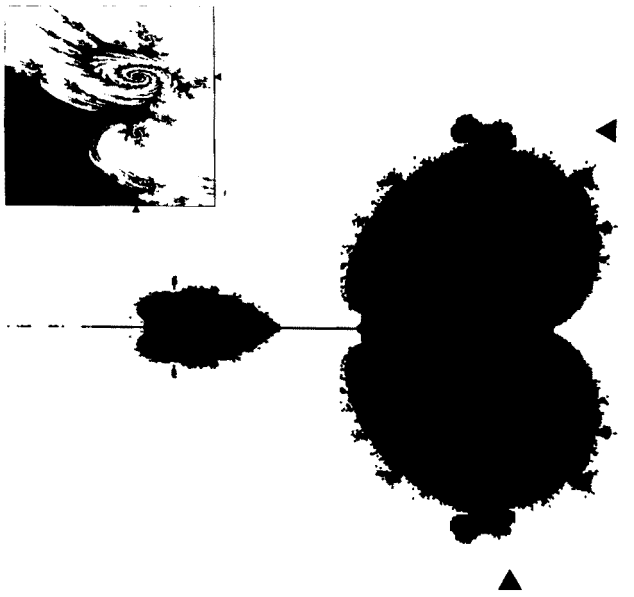

Fig. 5. "Generalized Mandelbrot set" for equation (5) with the same parameter for c_{re} and c_{im} plane like in Fig. 2. The inset shows a magnification of a detail close to the region indicated by the black markers at the frame of the image. This parameter corresponds to the values used to evaluate Fig. 3; after [12].

following nonanalytic map [16],

$$u(x,y) = 2xy - y^2 + a - b/\sqrt{3},$$
$$v(x,y) = 2xy - x^2 + a - b/\sqrt{3}. \tag{6}$$

That this is just a transformation of the complex equation (1) destroying the analyticity but uneffecting the dynamical properties and the structure is discussed in Ref. [17,18].

4. A generic mechanism for fractal boundaries

So far, we have presented some details of Julia and Mandelbrot sets and the role of analyticity. We showed that analyticity is not necessary to obtain these fractal structures. In the following, we present a simple model explaining how fractal boundaries are generated. This model is deduced from a simple mechanism which can easily be embedded in a mechanical

process. Well, we claim to have found an explanation of fractals in the spirit of Newton's understanding of nature.

The main idea is that a chaotic forcing applied to a bistable system can generically lead to fractal basin boundaries: see [19] for a generic differentiable example — a four-variable ordinary differential equation of chemical origin, [20] for a nongeneric example — a three-variable diffeomorphism containing a two-variable strictly Hamiltonian subsystem, and [21] for a generic example of a three-variable diffeomorphism. Fig. 6 illustrates the underlying principle. Due to the chaos present on the boundary (like it is also the case for the Julia set), two arbitrarily closely adjacent points on the boundary, with Δy arbitrarily small, are bound to become decorrelated in a finite time. It therefore appears plausible to conjecture that whenever the exponential divergence within the chaos (*i.e.*, its positive Lyapunov characteristic exponent) numerically exceeds the exponential escape from the boundary (*i.e.*, its locally unstable eigenvalue), the phenomenon of nowhere differentiability sets in.

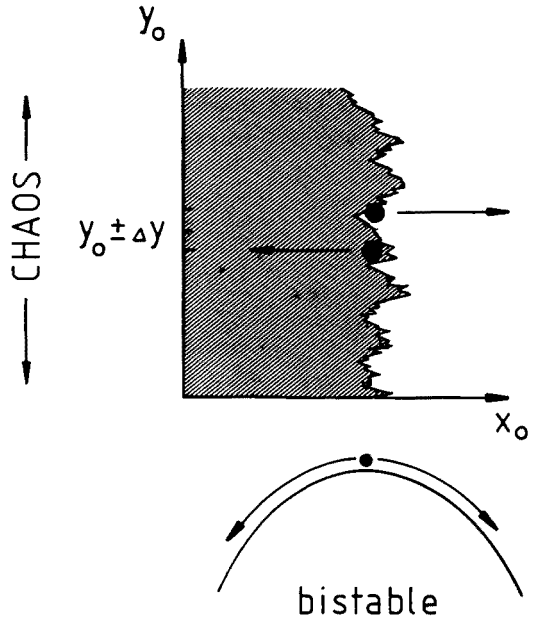

Fig. 6. Schematic view of the mechanism leading to a fractal basin boundary in the plane of initial conditions of a chaotically forced single-variable bistable system. Compare text for explanation.

This conjecture is to be clarified in the following, using a simple example. Consider the explicit generic diffeomorphic mapping in three variables

$$x_{n+1} = x_n^{\alpha} + by_n,$$

$$y_{n+1} = 3.95y_n(1 - y_n) + \varepsilon z_n,$$
$$z_{n+1} = x_n, \tag{7}$$

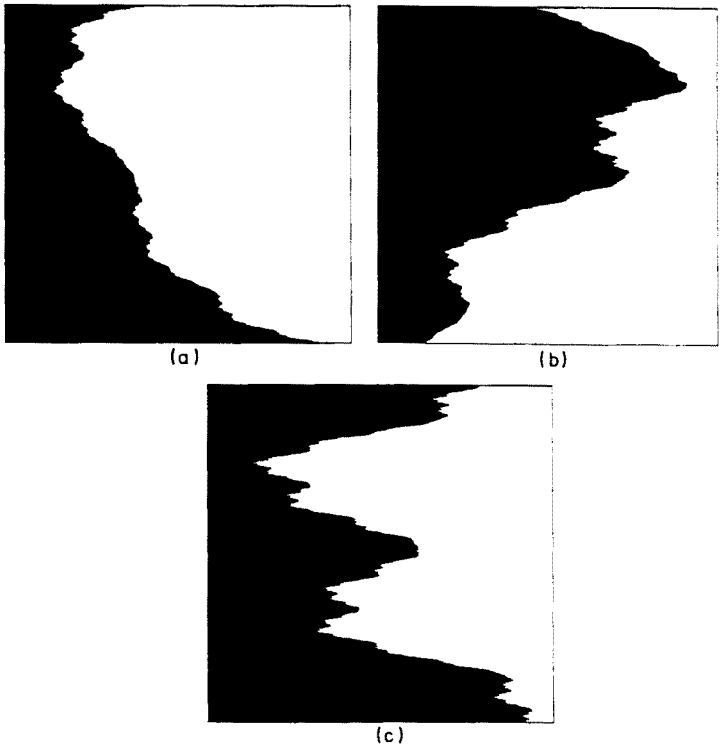

Fig. 7. A nowhere differentiable basin boundary in Eq. (7). Parameters: $\alpha = 1.95$, $b = 0.1, \varepsilon = 0.01, z_0 = 0$. (a) Coordinate frame of initial conditions (x_0, y_0). Coordinates lower left corner: $x_{\text{low}} = 0.9$, $y_{\text{low}} = 0.0$; window size: $\Delta x = 0.1$, $\Delta y = 1.0$. (b) Zoom of Fig. 7(a): $x_{\text{low}} = 0.91409567$, $y_{\text{low}} = 0.74545$; window size: $\Delta x = 10^{-6}$, $\Delta y = 10^{-5}$. (c) Zoom of Fig. 7(b): $x_{\text{low}} = 0.914095690964689$, $y_{\text{low}} = 0.74545021396629$; window size: $\Delta x = 10^{-12}$, $\Delta y = 10^{-11}$. Criteria for coloring: $x_n < 0.1$ black, $x_n > 1.0$ white. Grid size 500 × 500 pixels; after [21].

with x_n, y_n, z_n, α, b being real numbers, $n = 1, 2, ..., N$, and ($\alpha > 1$, $0 < b < 1$, $\varepsilon << 1$). The first variable is the bistable system forced by the chaotic subsystem (second variable) based on the logistic equation. The third variable serves, together with the weak coupling term ε in the second line, to render the whole system differentiable and invertible (that is, a diffeomorphism). The Jacobian determinant is a constant, equalling $b\varepsilon$. A numerical calculation using the familiar staining technique (*i.e.*, basins

of the finite attractors are colored black, initial conditions escaping to infinity are left white) is presented in Fig. 7. Two magnifications are shown, differing in linear scale by a factor 10^{12}. Numerically, the impression of a self-similar, nowhere differentiable basin boundary appears to be justified.

Under the simplifying assumption of ϵ being equal to zero, the boundary of Fig. 7(a) is replotted in Fig. 8. Fig. 8(a) gives the numerical visualization of the basic idea demonstrated in Fig. 6. The explosion criterion "x larger than unity" has been chosen. A glance at equation (7) shows that with initial conditions $0 < y_0 < 1$ the chaotic forcing is positive definite. Therefore, an explosion criterion for the boundary $x \geq 1$ is justified because any $x_n \geq 1$ will increase under iteration. Figure 8(b) shows the same picture as Fig. 8(a), yet with "level lines" dependent on the number of iterations after which the explosion criterion was fulfilled. The level lines approaching the basin boundary add up to a progressive sequence and correspond to the elements of a Weierstrass-like function (*cf.* [22] and Voss in [7]).

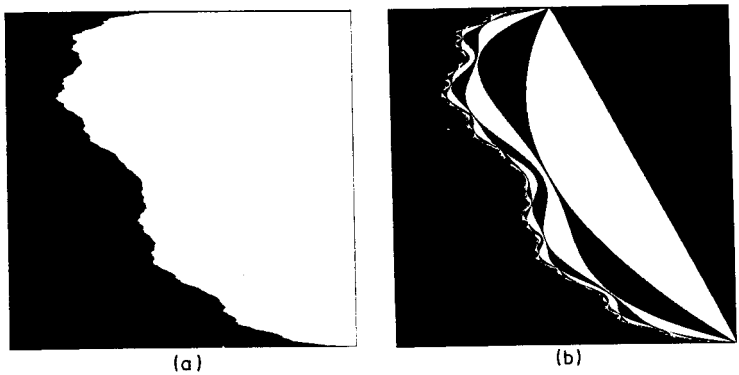

Fig. 8. (a) The same boundary as in Fig. 7(a) for the special case $\epsilon = 0$ in Eq. (7). (b) The same as Fig. 8(a) with "level line" entered. See text for an explanation; after [21].

This impression can be formalized. For example, all points, which fulfill the condition

$$x_1 \geq 1, \tag{8}$$

after one step, lie within the white "triangle" of Fig. 8(b). When interpreted in terms of the initial condition (x_0, y_0), condition (8) translates into

$$x_0^{(1)} \geq (1 - by_0)^{1/\alpha}, \tag{9}$$

with x_0, y_0, α, b being real numbers. $x_0^{(1)}$ means the first iterate of the initial point x_0. To derive analytic expression for the successive level lines,

we write Eq. (7) with $\varepsilon = 0$ in the general form

$$\begin{aligned} x_{n+1} &= F(x_n) + by_n, \\ y_{n+1} &= G(y_n). \end{aligned} \tag{10}$$

In our case, the function $F(x_n) = x_n^{\alpha}$ defines the bistable boundary with an unstable fixed point at $x = 1$ and the function $G(y_n) = 3.95y_n(1 - y_n)$ the bounded fixed chaotic forcing with $0 < y_n < 1$. With these conventions, Eq. (9) translates into

$$x_0^{(1)} \geq F^{-1}(1 - bG^{(0)}), \tag{11}$$

where $x_0^{(1)}$ is the first iterate of the initial condition x_0 which fulfills condition (8), $F^{-1}(1 - bG^{(0)})$ is the inverse function of F with the argument $(1 - bG^{(0)})$, and $G^{(0)}$ is the zero iterate, resp. the initial condition y_0.

All initial conditions which fulfill the explosion criterion after two iterations lie within the black parabolic segment of Fig. 8(b). The explicit analytic expression of this set reads

$$x_0^{(2)} \geq F^{-1}(F^{-1}(1 - bG^{(1)}) - bG^{(0)}).$$

For the n-th iterate, we analogously obtain

$$x_0^{(n)} \geq F^{-1}(F^{-1}(\cdots F^{-1}(1 - bG^{(n-1)}) - bG^{(n-2)}) \cdots - bG^{(1)}) - bG^{(0)}), \tag{12}$$

with the conventions $G^{(n)} = G^{(n)}(y_0)$ and $G^{(0)} = y_0$. Again, $G^{(n)}$ means the n-th iterate of the function G. The general condition (12) holds true for every function F in Eq. (10) which is invertible in a (sufficiently large) neighborhood of the unstable fixed point and every function G generating a bounded chaos confined to $0 < G < 1$. The equation corresponds to the borderline as n goes to infinity.

We are now in the position to return to Fig. 8. The curves seen there correspond to the set of functions described by Eq. (12). Since each level line strictly exceeds the preceding one, it is possible to speak of the limiting function (for n to infinity) as a Weierstrass-like function. Accordingly, Eq. (12) might be interpreted as an "iterative procedure" for a generation of Weierstrass-type functions.

Weierstrass-like functions generate "self-affine" behavior [1,22]. There are always two essential parameters involved. Their ratio determines whether genuine self-similarity as a special case of self-affinity or whether genuine (nondegenerate) self-affinity applies. In our case, these parameters correspond to the Lyapunov characteristic exponent of the chaotic forcing and the exponent of divergence from the bistable boundary.

There are two possibilities, the "striped" case and the "smooth" case. The former has infinite slope of both positive and negative sign in every point (ordinary Weierstrass-type nowhere differentiability) in the limit. The latter is smooth in the sense that in every point the l.h.s. and the r.h.s. limits of the slope differ only by infinitesimal deviation. The genuinely self-similar special case (ratio of unity) falls into the Weierstrass-type category, only that the slope in every point is finite.

These three cases that are implicit in Eq. (12) can indeed be found empirically in Eq. (7). The self-similar case has already been presented in Fig. 7. The two remaining cases are displayed in Figs. 9 and 10.

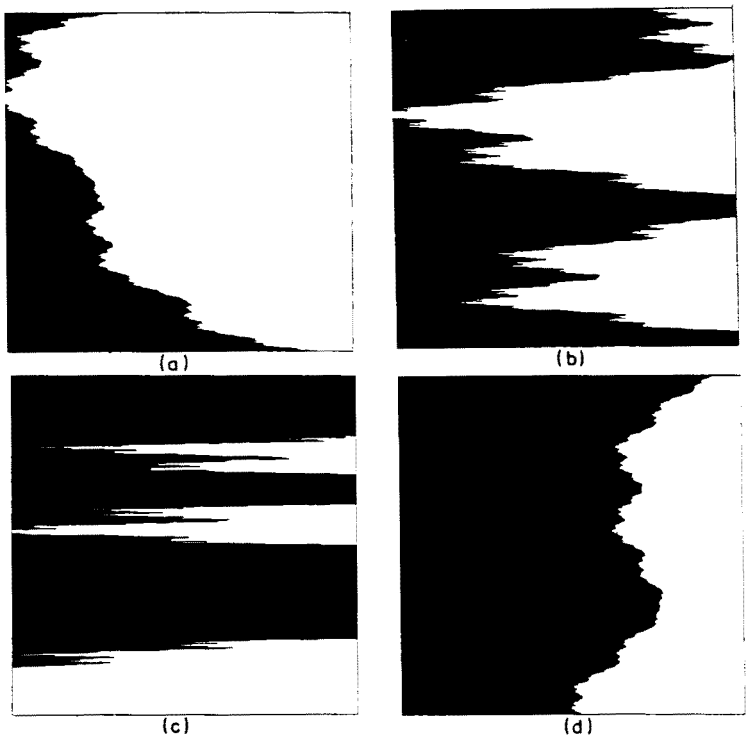

Fig. 9. Basin boundary in Eq. (7) calculated as Fig. 8. Parameters: $\alpha = 1.8, b = 0.1, \varepsilon = 0.01, z_0 = 0$. (a) Coordinate frame of initial conditions (x_0, y_0). Coordinates lower left corner: $x_{\text{low}} = 0.9$, $y_{\text{low}} = 0.0$; window size: $\Delta x = 0.1$, $\Delta y = 1.0$. (b) Zoom of Fig. 9(a): $x_{\text{low}} = 0.9006$, $y_{\text{low}} = 0.72$; window size: $\Delta x = 10^{-4}$, $\Delta y = 10^{-3}$. (c) Zoom of Fig. 9(b): $x_{\text{low}} = 0.9006225$, $y_{\text{low}} = 0.720135$; window size: $\Delta x = 10^{-6}, \Delta y = 10^{-5}$. (d) Affine rescaling of Fig. 9(c). Squeezing factor along x-axis: 20; after [21].

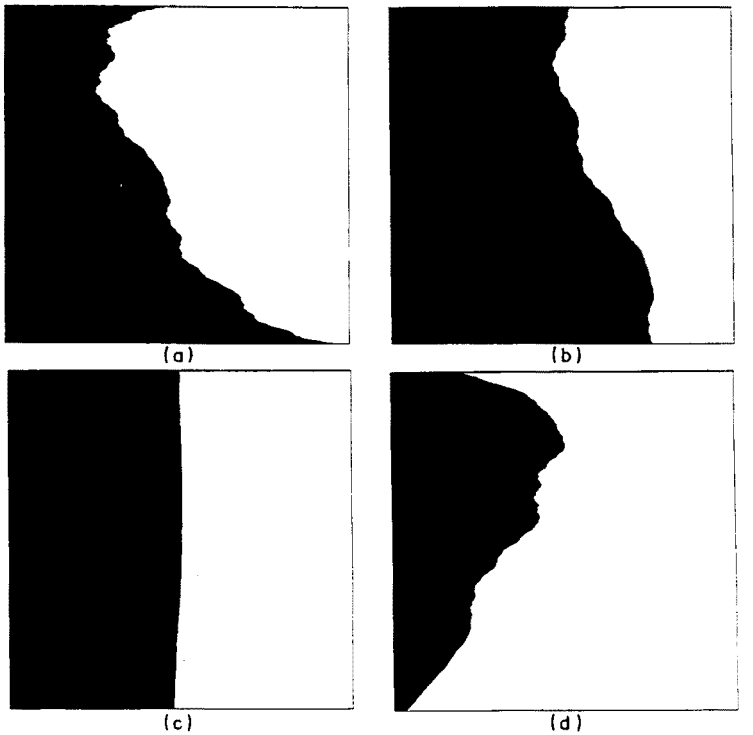

Fig. 10. Basin boundary in Eq. (7) calculated as Fig. 8. Parameters: $\alpha = 2.1, b = 0.1, \varepsilon = 0.01, z_0 = 0$. (a) Coordinate frame of initial conditions (x_0, y_0). Coordinates lower left corner: $x_{\text{low}} = 0.9$, $y_{\text{low}} = 0.0$; window size: $\Delta x = 0.1$, $\Delta y = 1.0$. (b) Zoom of Fig. 10(a): $x_{\text{low}} = 0.947055$, $y_{\text{low}} = 0.4523$; window size: $\Delta x = 10^{-5}$, $\Delta y = 10^{-4}$. (c) Zoom of Fig. 10(b): $x_{\text{low}} = 0.9470625399$, $y_{\text{low}} = 0.452304147$; window size: $\Delta x = 10^{-10}$, $\Delta y = 10^{-9}$. (d) Affine rescaling of Fig. 10(c). Squeezing factor along y-axis: 20; after [21].

To prove the conjecture, it was argued by Christen [23] and independently by Okninsky [24] to take the function F linear, so that $F^{-1}(y) = 1/m$, where m is the slope of F. This allows to rewrite Eq. (12) in the following way

$$x_0^{(n)} \geq -\left(\frac{b}{m}\right) \sum_n \frac{G^{(n)}}{m^n}. \tag{13}$$

This form is already very close to the Weierstrass function. Another trial to prove the conjecture is given in [25], where the added structure of the

"level lines" (see Fig. 8) are estimated in size. From this the local derivative is deduced.

5. A model for turbulent and intermittent structures

Next, we interpret the results mentioned above in a different way. To obtain a fractal line we will stick only to the explicit asymptotic Eq. (12). We already know that this fractal curve is created by a process of successively adding further and further structures to an initially simple and smooth curve. In Fig. 11, the added structures of the first 5 levels are shown. Here, we calculated the differences between two successive level lines, see Fig. 8, by evaluating $x_0^{(n)} - x_0^{(n-1)}$ of Eq. (12). These successively added structures represent something like the Weierstrass components of the final fractal curve.

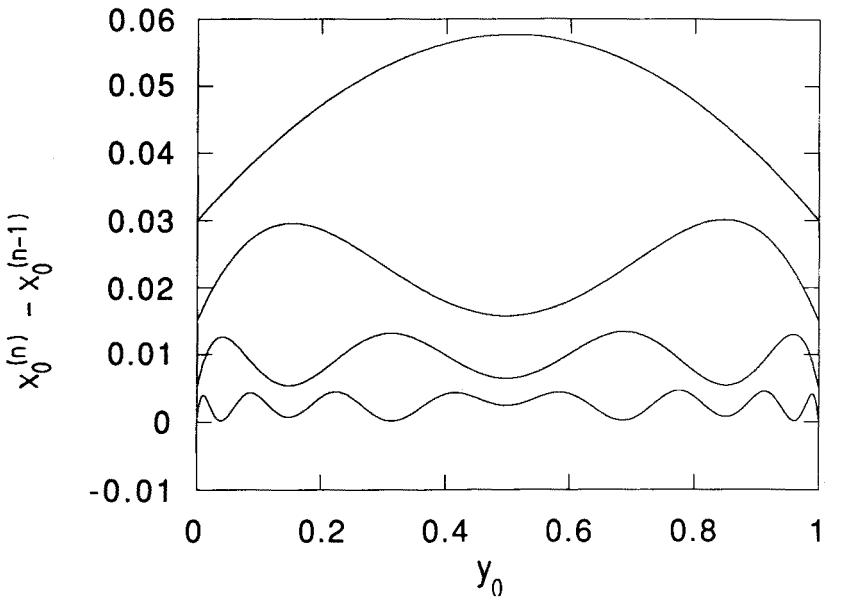

Fig. 11. Added structure of the n-th iterate, constructed from the differences between the first level lines of Fig. 8b. From top to bottom, curves of $(x_0^{(n)} - x_0^{(n-1)})$ *vs.* y_0 using Eq. (12) are shown for $n = 2, 3, 4$, and 5. For clarity, the curves are shifted so that they do not intersect.

This successive process may be taken as a "structure adding machine". Eq. (12) tells us that the added structure of the next level is characterized by a further term in G and F^{-1}, *i.e.*, by one further application of a chaotic stretching and an inverse bistable stretching, which is nothing else than a folding. This is taken as a natural (physical) process evolving in time. The interpretation is that a system starts with some homogeneous structure in y_0 direction (a space coordinate for example). The result of the first application of the stretching G and folding F^{-1} is a structure with one maximum (see Fig. 11). The next iterations will add more and more local maxima and lead finally to the fractal curve.

To make this idea more concrete, let us take an initially laminar gaseous jet which becomes turbulent with propagation. For this gaseous jet, we consider a spatial part, which is now our y_0 direction. We denote the velocity in this spatial part with $x_0^{(n)}$. Here, n denotes the time of propagation and, thus, the time of developing turbulence. The level lines of Fig. 8 or Fig. 11 correspond to velocity fluctuations developing in time. First, a structure with one maximum is generated, then successively further maxima are added, and finally a fractal velocity fluctuation curve is obtained in space. The fractality of this velocity function corresponds to the famous $1/f$ noise in turbulence. A maximum and a minimum of one iteration level, in the sense of added structure of Fig. 11, can be interpreted as a measured velocity fluctuation through vorticities of one shell. Thus, Fig. 11 presents a vortex cascade. The number of vorticities increases here by a factor 2 by each step (going from n to $n+1$). At the same time, the size (distance between neighboring maxima and minima in y_0 direction) of the vortex decreases. This interpretation has similarities to the Richardson cascade of turbulence.

One essential point of our model is that we take care of the different initial conditions in y_0 space. The different initial conditions develop under the iteration by the chaotic map. The sensitive dependence of the chaos, *i.e.*, the positive Lyapunov exponent, creates the fractal spatial structure. The Ansatz can be seen as a new method to explain spatio-temporal structures, in contrast to the common approach of spatial coupling of many dynamical subsystems. In our model, no interaction between two spatially neighboring points (initial y_0 points) is considered so far. But in principle it is easily done, and perhaps it is of importance to model such effects like those known from the dissipative range in turbulence, where spatial viscous interaction causes a smoothing out of the vortex cascade, *i.e.*, a smoothing out of the fractal structure.

A further point of our model is that multifractal structures are evidently present. Here, one has only to note that different initial conditions of y_0 have slightly different chaotic trajectories, and thus different effective Lya-

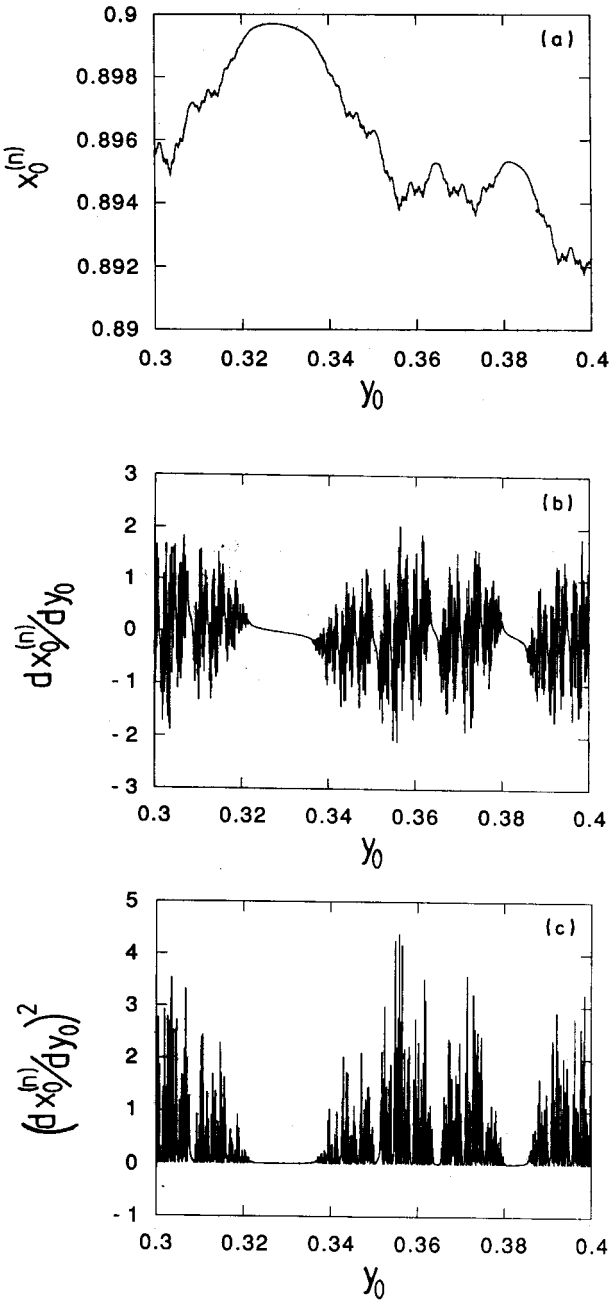

Fig. 12. Graph of Eq. (12) for $F = x^{1.6}$, $G = 3.83y(1-y)$, $b = 0.1$, and $n = 50$. (a) The original curve is shown for $0.3 < y_0 < 0.4$. There is no deeper meaning behind this choice of the y_0 regime. (b) Derivative of Fig. 12(a); and (c) the square of the derivative of Fig. 12(a).

punov exponents are obtained as a function of the initial conditions. These fluctuations in the Lyapunov exponents cause different local fractal structures, *i.e.* multifractal structures, as it becomes clear by our conjecture of the previous part. (Multifractality is of special interest in turbulence [25].)

As a last point, some intermittency effects are discussed. Fractals in nature are very rarely everywhere fractal, but it is much more common to find smooth and fractal sections in a disordered way close to each other. Here, for example, we have in mind the typical structure of some mountains, like the Tatry. Rocky fractal parts are well mixed with smooth meadows. In turbulence, this effect is known as high frequency intermittency. To model such structures, we were inspired by the work of Okninsky [26] who showed and told us that intermittency effects can be generated if one uses transient chaos. In Fig. 12, the obtained fractal structure is shown for transient chaos (the parameters for G were taken for the period three window of the logistic map). To make the intermittent structure more evident, we calculated the derivative and the square of the derivative of this curve. Well, the square of the derivative has some special meaning in turbulence. If we take the original structure (Fig. 12(a)) as the velocity in space, the square of the derivative of the velocity corresponds to the local dissipated energy. Finally, we should point out that we do not claim to have found the solution of modelling and explaining turbulence, but we want to stress that with this simple model some new insight into the structure formation in nature can be deduced. There are probably many other systems where this process of chaotic stretching and folding can explain the structure formation. Taking the added structure of Fig. 11 for example as some deposition of mattern, it may become possible to describe surface growth phenomena. One fascinating point of our model is that only some new interpretation of deterministic and low dimensional chaos is presented here.

6. Summary

We have shown the role of analyticity for fractals. By perturbations and a transformation of the complex analytic function we showed that analyticity is not necessary for fractals. With the example of a chaotic forced bistability we have presented a simple mechanism leading to different kinds of fractality. Depending on the strength of chaos and bistabitity, which can be measured by two characteristic exponents, it was shown how self-affine, self-similar, and nowhere-differentiable structures are obtained. The result of self- similarity was due to the equality of the two characteristic exponents. Taking into account that the Chauchy–Riemann condition garantees the equality of these exponents, the beauty of complex analytic fractals becomes clearer. The uniqueness of the basin boundary function of the model

of a chaotic forced bistability allowed us to deduce an explicit function for the boundary. With this function, the connection to the Weierstrass function has been shown. Thus, our model enabled us to show the relation between chaos, fractal boundary, and Weierstrass function ($1/f$ noise).

As a last consequence, we have presented a new interpretation of the model of chaotic forced bistability, leading us to a structure generating process. Fractality is achieved by the iterative application of chaotic stretching and folding. We discussed the possibility to explain some phenomena known from hard turbulence. One essential new point is that deterministic chaos causes out of the infinity of different initial conditions complicated fractal structure formation.

For helpful discussions we want to thank G. Baier, R. Stoop, and A. Okninsky. For financial support J. Peinke wants to thank the Deutsche Forschungsgemeinschaft.

REFERENCES

[1] B.B. Mandelbrot, *The Fractal Geometry of Nature*, ed. W.H. Freeman, New York, 1982.
[2] G. Julia, *J. Math. Pure at Appl.* **4**, 47 (1918).
[3] P. Fatou, *Bull. Soc. Math. France* **47**, 161 (1919).
[4] H.-O. Peitgen, P.H. Richter, *The Beauty of Fractals* Springer-Verlag, Berlin, 1986.
[5] R.L. Devany, *An Introduction to Chaotic Dynamical Systems* Benjamin/Cummings, Menlo Park, 1986.
[6] P. Blanchard, *Bull. Americ. Math. Soc.* **11**, 85 (1984).
[7] H.-O. Peitgen, D.Saupe (eds.), *The Science of Fractal Images*, Springer-Verlag, Berlin, 1988.
[8] K.-H. Becker, M. Dörfer, *Dynamical Systems and Fractals*, Cambridge University Press, Cambridge, 1989.
[9] J. Feder, *Fractals*, Plenum Press, New York, 1988.
[10] M. Klein, O.E. Rössler, J. Parisi, J. Peinke, G. Baier, C. Kahlert, J.L. Hudson, *Comput. and Graphics* **15**, 583 (1991).
[11] C. Kahlert, O.E. Rössler, *Z. Naturforsch.* **42a**, 324 (1987).
[12] J. Peinke, J. Parisi, B. Röhricht, O.E. Rössler, *Z. Naturforsch.* **42a**, 263 (1987).
[13] J. Peinke, J. Parisi, B. Röhricht, O.E. Rössler, W. Metzler, *Z. Naturforsch.* **43a**, 14 (1988).
[14] J. Peinke, J. Parisi, B. Röhricht, O.E. Rössler, *Z. Naturforsch.* **43a**, 287 (1988).
[15] B. Röhricht, W. Metzler, J. Parisi, J. Peinke, W. Beau, O.E. Rössler, *The Classes of Fractals*, in *The Physics of Structure Formation - Theory and Simulation*, eds. W. Güttinger and G. Dangelmayr, Springer Verlag, Berlin, 1987, p.275.

[16] M. Klein, *Z. Naturforsch.* **43a**, 819 (1988).
[17] C. Kahlert, M. Klein, *Z. Naturforsch.* **43a**, 1091 (1988).
[18] W. Metzler, A. Brelle, K.-D. Schmidt, *Non Analytic Dynamics generating the Mandelbrot Set*, Mathematische Schriften Kassel, Gesamthochschule Kassel, Preprint No. 8/91, Juni 1991.
[19] O.E. Rössler, J.L. Hudson, M. Klein, *J. Phys. Chem.* **93**, 2858 (1989).
[20] C. Grebogi, E. Ott, J.A. Yorke, *Physica* **7D**, 181 (1983).
[21] J. Peinke, M. Klein, A. Kittel, G. Baier, J. Parisi, R. Stoop, J.L. Hudson, O.E. Rössler, *Europhys. Lett.* **14**, 615 (1991).
[22] T. Tel, *Z. Naturforsch.* **43a**, 1154 (1988).
[23] Th. Christen, preprint (Basel 1990).
[24] A. Okninsky, private communication.
[25] J. Peinke, M. Klein, A. Kittel, C. Kahlert, R. Stoop, J. Parisi, O.E. Rössler, *Bifurcation and Chaos* (in press).
[25] U.Frisch and St.A. Orszag, Physics Today, January 1990, p.24
[26] A. Okninsky, *J. Stat. Phys.* **52**, 577 (1988).